Article

Failure of *Micractinium simplicissimum* Phosphate Resilience upon Abrupt Re-Feeding of its Phosphorus-Starved Cultures

Elena Lobakova [1,2‡], Olga Gorelova [1‡], Irina Selyakh [1], Larisa Semenova [1], Pavel Scherbakov [1], Svetlana Vasilieva [1,2], Petr Zaytsev [1,2], Karina Shibzukhova [1], Olga Chivkunova [1], Olga Baulina [1], and Alexei Solovchenko [1,2*]

[1] Department of Bioengineering, Faculty of Biology, Lomonosov Moscow State University, 1-12 Leninskie Gory, 119234 Moscow, Russia; i-savelyev@mail.ru (I.S.), semelar@mail.ru (L.S.), elena.lobakova@gmail.com (E.L.), cyano@mail.ru (P.S.), vankat2009@mail.ru (S.V.), zaytsevpa@mymsu.ru (P.Z.), shibzukhova.karina@yandex.ru (S.K.), olga.chivkunova@mail.ru (O.C.), baulina@inbox.ru (O.B.), ogo439@mail.ru (O.G.), solovchenkoae@my.msu.ru (A.S.)

[2] Institute of Natural Sciences, Derzhavin Tambov State University, Komsomolskaya Square 5, 392008, Tambov, Russia

* Correspondence: solovchenkoae@my.msu.ru; Tel.: +7(495)939-35-87

‡ These authors equally contributed to this work.

Abstract: Microalgae are naturally adapted to fluctuating availability of phosphorus (P) being capable to opportunistically uptake large amounts of inorganic phosphate (P_i) and safely store it in the cell as polyphosphate. Hence, many microalgal species are remarkably resilient to high concentrations of external P_i. Here we report on an exception from this pattern comprised by a failure of the high P_i-resilience in a strain *Micractinium simplicissimum* IPPAS C-2056 normally coping with a very high P_i concentrations. This phenomenon occurred after abrupt re-supplementation of P_i to the *M. simplicissimum* culture pre-starved of P. This was the case even if P_i was re-supplemented in a concentration far below the level toxic to the P-sufficient culture. We hypothesize that this effect can be mediated by a rapid formation of the potentially toxic short-chain polyphosphate following the mass influx of P_i into the P-starved cell. A possible reason for this is that the preceding P starvation impairs the capacity of the cell of converting the newly absorbed P_i into a "safe" storage form of long-chain polyphosphate. We believe that findings of this study can help to avoid sudden culture crashes, they are also of potential significance for development of algae-based technologies for efficient bioremoval of P from P-rich waste streams.

Keywords: *Micractinium*; inorganic phosphate; polyphosphate; phosphorus toxicity

1. Introduction

Phosphorus (P) is a major nutrient central to the processes of energy and information storage and exchange in cell [1-3]. Most of the habitats accessible to microalgae are characterized by variable availability of P [4,5], but inorganic P species (referred to below as P_i) are usually present at limiting concentrations [6-8]. To withstand prolonged P shortage, microalgae developed a set of adaptations collectively called "luxury uptake" [6,7]. The latter includes the capability of absorbing P_i in amounts much greater than their metabolic demand [9]. Another set of mechanisms converting the newly acquired P_i into relatively metabolically inert polyphosphate (PolyP) and store it into the cell vacuole serve to avoid fatal displacement of the equilibria of vital metabolic reactions in which P_i participates [1,3].

Possibly as a side effect of these adaptations, microalgae became remarkably resilient to high levels of external P_i by far exceeding its environmental concentrations (1 g L^{-1} and more [10]). Some microalgal species found in P-polluted sites display very high P_i tolerance (see e.g. [10]). It makes microalgae a powerful vehicle for biocapture of P from waste streams [11] increasing thereby sustainability of using P resources which is currently notoriously low (< 20%) [12]. Indeed, there are numerous reports on successful use of microalgae exerting luxury uptake of P [13,14] for biotreatment

 doi:10.20944/preprints202304.0688.v1

of waste streams to avoid eutrophication [12,15] and produce environmentally friendly biofertilizers [16,17].

From the practical view, microalgae-based approaches for P biocapture from waste streams offer advantages conventional techniques such as EPBR [2,18]. Using waste- and side-streams as P source for industrial cultivation of microalgae makes the bulk bioproducts such as P biofertilizers [16,19] or biofuels economically viable [20]. Biomass of microalgae is a potential source of PolyP that can be used in medicine, for the development of biomaterials, and in food industry [21,22].

Despite the promise of microalgae-based P capture, its use is hindered by insufficient knowledge of luxury P uptake mechanisms [1,3] and the lack of strains resilient to high concentration of P_i since many algal species commonly used in biotechnology can be inhibited already at P_i concentration above 0.1–0.3 g L^{-1} [23,24].

Nevertheless, there are reports on the toxicity of exogenic P_i to microalgae [23-25] although the mechanisms of this phenomenon a far from being understood. Still, understanding of P toxicity is important e.g. for development of viable biotechnologies for the nutrient biocapture from P-rich waste streams and/or the highly nutrient-polluted sites. To further bridge this gap, we investigated failure of high P resilience in P-starved cultures. The *Micractinium simplicissimum* strain IPPAS C-2056 recently isolated from a P-polluted site served as a model organism for this study. The cultures of the *M. simplicissimum* grown in P-replete media exhibit a very high P_i-resilience [10]. In our recent experiments on P starvation, we observed a sudden culture death upon replenishment of Pi to the P-depleted culture of the *M. simplicissimum*. Here, we report on the effect of abrupt increase of the external P_i on the cell viability, P_i uptake, internal content of P and PolyP. We elaborate on possible mechanisms of P_i-induced death of microalgal cells acclimated to P deficiency. Special attention was paid to the potential role short-chain PolyP in these mechanisms.

2. Results

To test the effect of P starvation with subsequent P_i replenishment on the *M. simplicissimum* culture condition, the P-sufficient culture was deprived of P for 14 d, then P_i was replenished to the medium and the culture was monitored for another 10 d (see Materials and Methods).

2.1. The dynamics of the culture condition during phosphorus starvation and re-feeding

During 14 days of P-deprivation, the precultures gradually changed their color from green to yellow green (Figure 1) which is typical of nutrient-deprived cultures responding to the stress by reduction of their photosynthetic apparatus. During first week of P deprivation, the culture exhibited a vigorous cell division commensurate to that commonly observed in P-replete cultures of the *M. simplicissimum*. The P-deprived cultures demonstrated the onset of stationary phase due to the P limitation by the 10th day of incubation. The P_i was replenished to the P-deprived cultures to the final concentration of 0.8 g L^{-1} which is far below the level potentially toxic to the *M. simplicissimum* [10]). The pH of the cultures remained in the range 6.7–7.7 throughout the experiment, so the Pi added to the cultures is expected to be readily available for the uptake by the microalgal cells. Our analysis of the absorbance spectra of the P-deprived cultures (Figure 2) revealed an increase in the relative contribution of the absorption of pigments in the blue-green region of the visible part of the spectrum which is consistent with the increase in carotenoid-to-chlorophyll ratio (not shown) observed in this culture manifesting itself as the changes in coloration described above (see also Fig. 1 **b**).

The absorbance spectra recorded for the first 24 h after P_i replenishment revealed a synchronous increase of the light absorption by the culture in the blue and red regions of the spectrum (Figure 2, curves *1* and *2*) attributable to the accumulation of pigments and balanced culture growth. Upon 24 h from P_i replenishment, the cultures started to show the visual signs of damage such as discoloration and increased turbidity indicative of the presence of cell debris. The corresponding absorbance spectra revealed a profound bleaching of the photosynthetic pigment absorption bands (Figure 2, curves *3-5*). The cultures became whitish by the 10th day of cultivation (Figure 2). At the same time the red absorption band of chlorophyll became undetectable on the spectra of the cultures although the small peaks attributable to the absorption by carotenoids remained (Figure 2, curve *5*). The

Preprints (www.preprints.org) | NOT PEER-REVIEWED | Posted: 21 April 2023 doi:10.20944/preprints202304.0688.v1

appearance and the optical properties of the cultures almost did not change thereafter. Overall, these observations evidenced the progressive lysis of the microalgal cells upon replenishment of P_i to the P-depleted cultures of the *M. simplicissimum*.

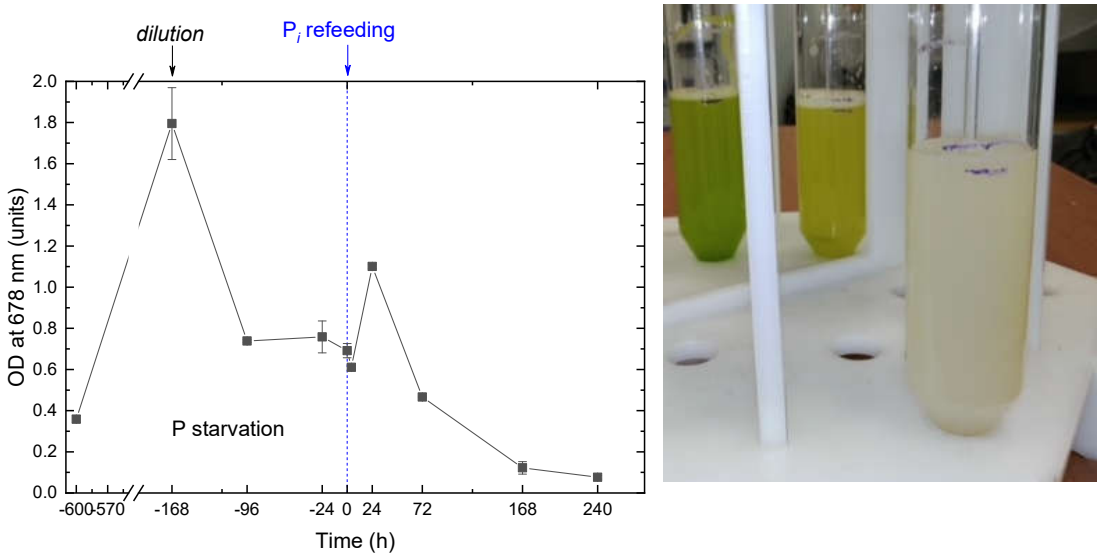

Figure 1. The changes in the *Micractinium simplcissimum* IPPAS C-2056 culture condition as manifested by (**a**) the kinetics of changes in the OD_{678} during its phosphorus starvation (negative time values) and after re-feeding of the P-starved cultures with P_i (positive time values). The moment of P_i re-feeding (t = 0 h) is marked on the graph by a vertical dashed line. (**b**) A typical visual appearance (left to right) of *Micractinium simplcissimum* IPPAS C-2056 (i) pre-culture; (ii) culture P-starved for 14 d, and (iii) the culture 168 h after re-feeding with P_i (see also Figure **2**). Cultures from different time-shifted replicas of the experiment running in parallel are shown in (**b**).

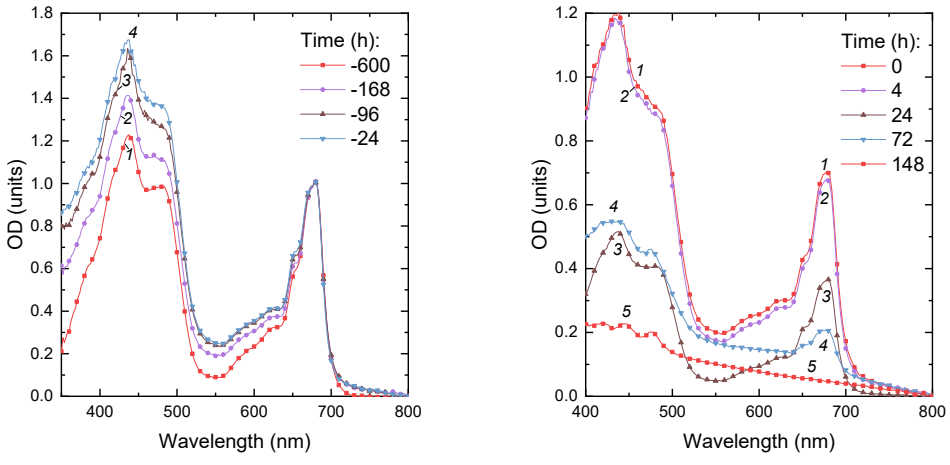

Figure 2. Changes in absorption spectra of the *Micractinium simplcissimum* IPPAS C-2056 cultures during **(a)** its P starvation and **(b)** after re-feeding of the pre-starved *Micractinium simplcissimum* IPPAS C-2056 cultures with P_i. The time of P starvation indicated in the panels (h) is counted down to the moment of P_i re-supplementation to the culture (t = 0 h; see Figure 1).

Preprints (www.preprints.org) | NOT PEER-REVIEWED | Posted: 21 April 2023 doi:10.20944/preprints202304.0688.v1

2.2. Phosphorus removal from the medium and its uptake by the cells

Monitoring of the removal of P_i after its replenishment to the P-deprived cultures showed that the most (75-80%) of the added P_i remained in the medium at all stages of the experiment (Figure 3). Around 3-5% of the added P_i has been adsorbed by the superficial structures of the *M. simplicissimum* cells as well as by cell debris were (see below); the amount of the adsorbed P_i was relatively constant. The amount of P_i taken up by the cells gradually increased during the first three days of the experiment but later it started to decline with the corresponding increase in the external P_i concentration (Figure 3). The increase of the residual P*i* in the culture likely reflected the release of P from the ruptured dead cells whose proportion increased in the culture, according to our observations outlined above.

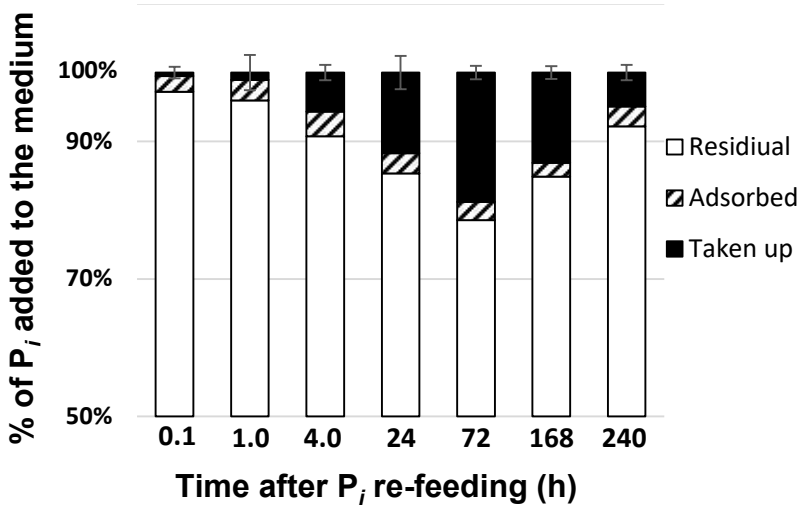

Figure 3. Changes in the distribution of the of the P_i which was either taken up or adsorbed by the cells of *Micractinium simplicissimum* IPPAS C-2056 or remained in the medium after re-feeding of P_i to the P-starved cultures (see Figure 1).

The analysis of the dynamics of the total intracellular P content revealed a rapid increase in the DW percentage of P from 0.25% typical of P-starved cells to 4% DW during the first 24 h after replenishment of P_i (Figure 4). The discrepancies between the trends shown in Figure 4 might stem from the difference in the techniques of sample processing (for details, see Methods). Another plausible reason is the shortage of metabolic resources of the cell available for the conversion of the incoming P_i to PolyP. Later this parameter declined to 1%, likely due to predominant lysis of the cells which took up the highest amounts of P_i.

The PolyP content of the cells also increased rapidly during the first hours after P_i replenishment, but it reached its maximum of 0.35% DW within ca. four hours and returned to the initial level of ca. 0.02% DW by the end of the first day of incubation of the culture under P-replete conditions. The PolyP cell content did not change significantly thereafter but showed a downward trend.

Preprints (www.preprints.org) | NOT PEER-REVIEWED | Posted: 21 April 2023 doi:10.20944/preprints202304.0688.v1

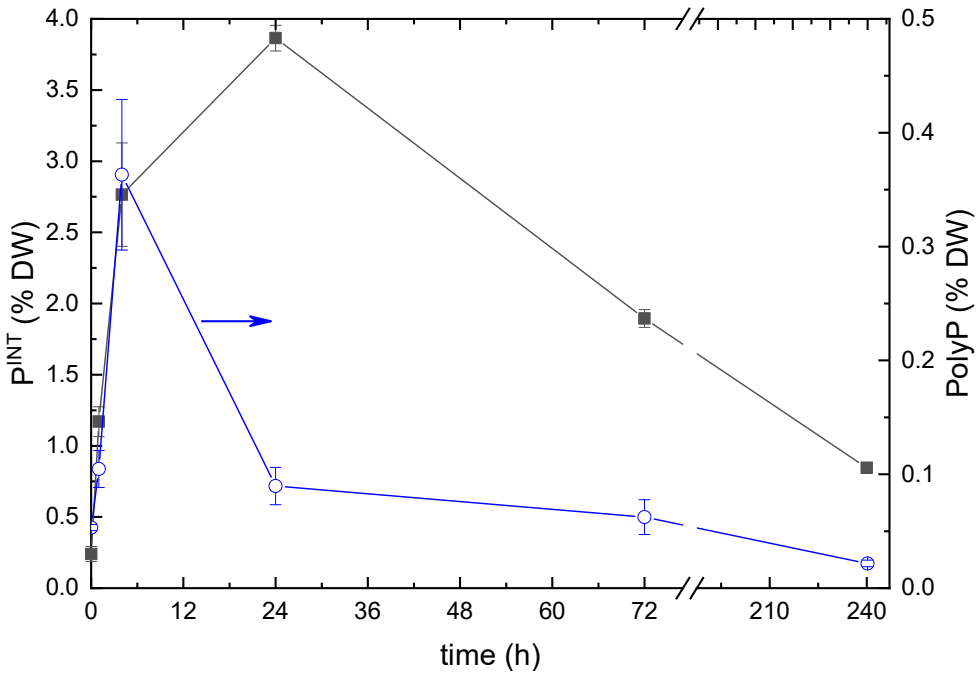

Figure 4. The changes in total intracellular P (left scale) and PolyP (right scale) contents in the cultures of *Micractinium simplicissimum* IPPAS C-2056 after re-feeding of the P-starved cultures with P_i.

2.3. Ultrastructural view of the changes in the cell P-pools

To gain a deeper insight into the rearrangements of P pools in the culture of the *M. simplicissimum* under our experimental conditions, an electron microscopy studies of cells sampled at the key stages of the experiment (see Figure 1) was carried out (Figures 5, A1, A2). The ultrastructure of the *M. simplicissimum* pre-culture cells was similar to that of the cells grown under similar conditions [10]. Briefly, the preculture consisted of individual round-shaped cells containing a single nucleus, parietal chloroplast with a centrally located pyrenoid; the culture also contained occasional autosporangia (Figures 5 **a** and 6 **a, b**). Empty envelopes of the autosporangia and cell walls of dead cells were also encountered in the culture (Figure 6).

The surface of the cells and autosporangia lacked bristles. The cell wall did not reveal the characteristic trilamellar pattern (sporopollenin- or algenat-like layer). Cell walls of live and dead mature cells and envelope of the autosporangia (but not the cell walls of the young cells) manifested, upon staining with DAPI, the yellow-green fluorescence indicative of the presence of PolyP (Figure 6 **b**).

Preprints (www.preprints.org) | NOT PEER-REVIEWED | Posted: 21 April 2023 doi:10.20944/preprints202304.0688.v1

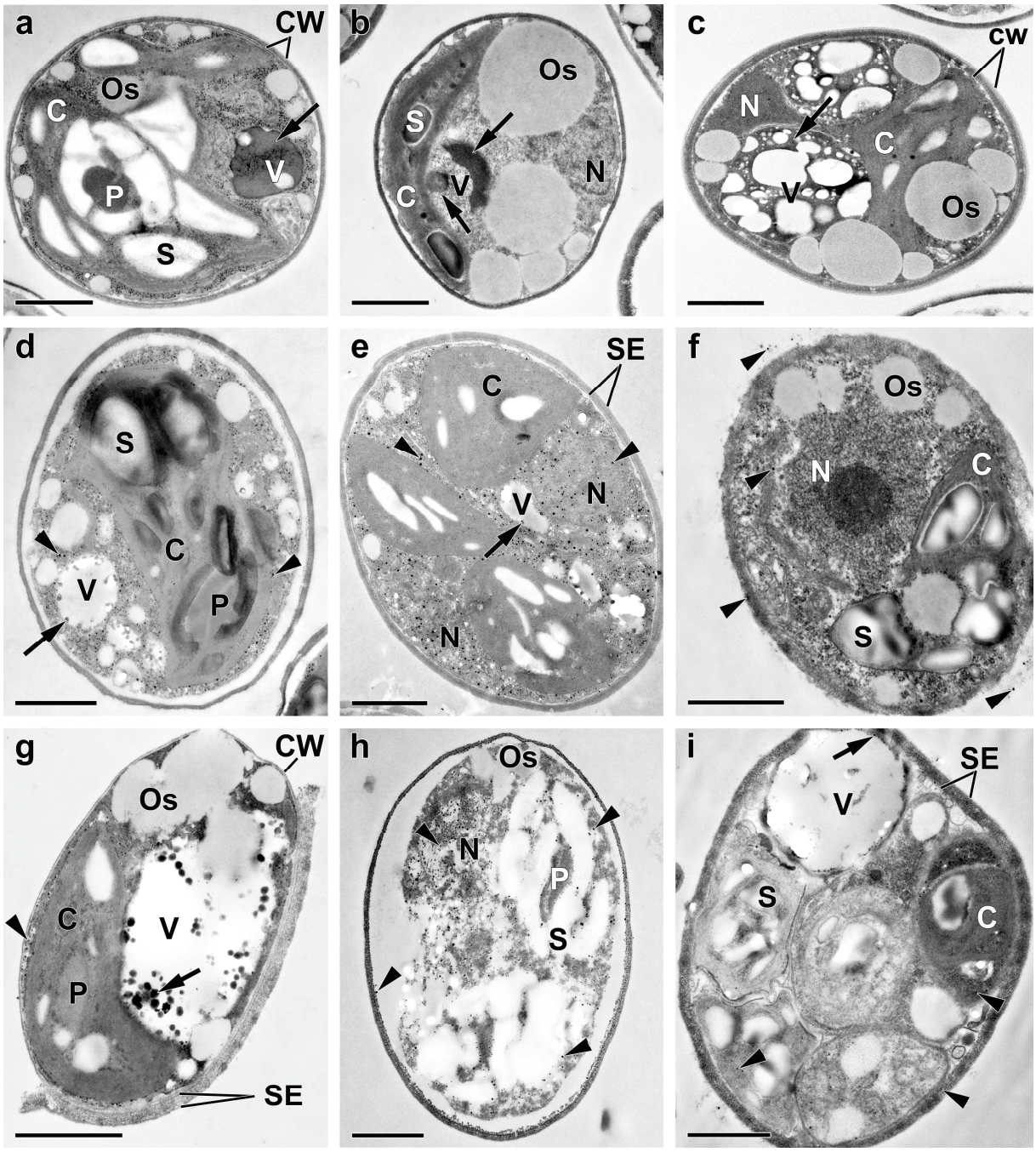

Figure 5. Typical transmission electron micrographs of cells (**a-d, f-h**) and autosporangia (**e, i**) of *Micractinium simplicissimum* IPPAS C-2056 reflecting their condition at different phases of the experiment (see also Figure 1). The micrographs of the culture in the BG-11$_K$ medium in glass columns, that were incubated constant bubbling with 5% CO_2 (**a**), P-starved cells (**b**), as well as of the cells (**a-d, f-h**) and sporangia (**e, i**) sampled 4 h (**c**), 24 h (**d, e**), and 72 h (**f-i**) after re-feeding of the P-starved cultures with P_i are shown. C, chloroplast, CW, cell wall, N, nucleus, Os, oleosome, P, pyrenoid, S, Starch granule, SE, sporangium envelope, V, vacuole. The arrows point to the inclusions in the vacuole. The arrowheads point to the electron-opaque particles on/in the cell wall and their adsorbed on the cell surface the clusters also to the spherules in the cytoplasm, the nucleus, and destructed chloroplast. Scale bars = 1 μm.

Preprints (www.preprints.org) | NOT PEER-REVIEWED | Posted: 21 April 2023 doi:10.20944/preprints202304.0688.v1

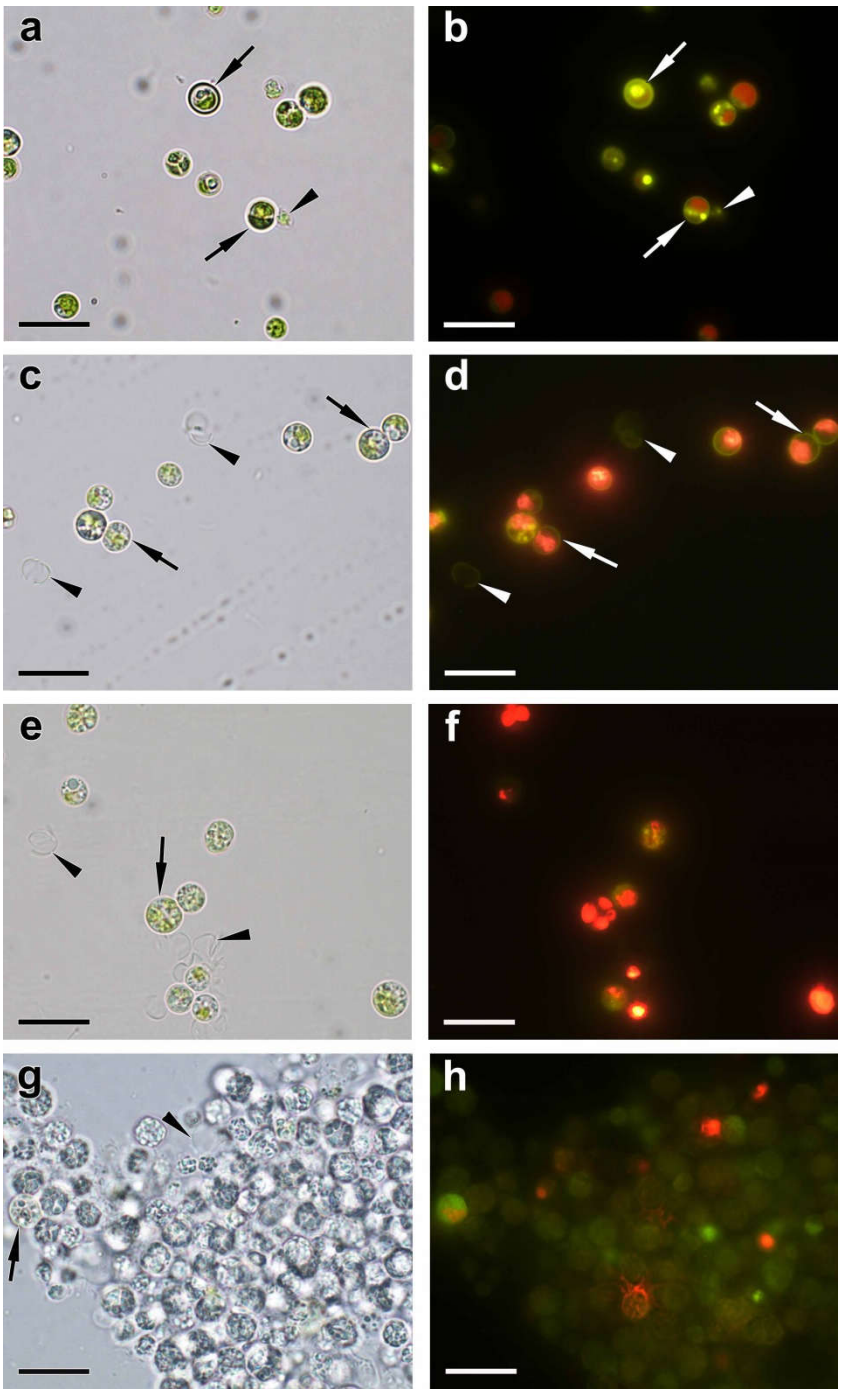

Figure 6. Typical brightfield (**a, c, e, g**) and fluorescent (**b, d, f, h**) microphotographs of DAPI-stained cells of *Micractinium simplicissimum* IPPAS C-2056 cells in pre-culture (**a, b**) and obtained 1 h (**c, d**), 24 h (**e, f**), and 168 h (**g, h**) after re-feeding of the P-starved culture with P_i. The arrows point to the cell wall. The arrowheads point to the cell debris including walls of the destructed cells. Scale bars = 20 μm.

The EDX spectra revealed P and iron in the cell walls as well as in the particles associated with them (Table A1). Carbon reserves were represented mainly by starch grains in the chloroplast (ca. 7.8 grains per cell section) and small (diameter 326 ± 18 nm, 986 nm max.) oleosomes (ca. 8 per cell section). Vacuoles contained spectacular inclusions—large round-shaped P-containing inclusions of non-uniform electron density (Figures 5a). Their EDX spectra possessed a distinct peak of P along with the characteristic peaks of nitrogen, calcium and magnesium (Table A1, Figure 7 **a**). The vacuoles also contained small roundish, electron-opaque inclusions harboring P or P in combination with uranium (see below and Table A1). Moreover, small electron-opaque spherules (10–40 nm in

Preprints (www.preprints.org) | NOT PEER-REVIEWED | Posted: 21 April 2023 doi:10.20944/preprints202304.0688.v1

diameter; 5–20 instances per cell section) of the same composition were detected in the cytoplasm (Figure A1 a, Table A1). Roundish inclusions were in the cells and in the sporangia. Roundish inclusions located in the cells and in the sporangia revealed, upon staining with DAPI, the PolyP-character yellow-green fluorescence (Figure 6 **a**, **b**).

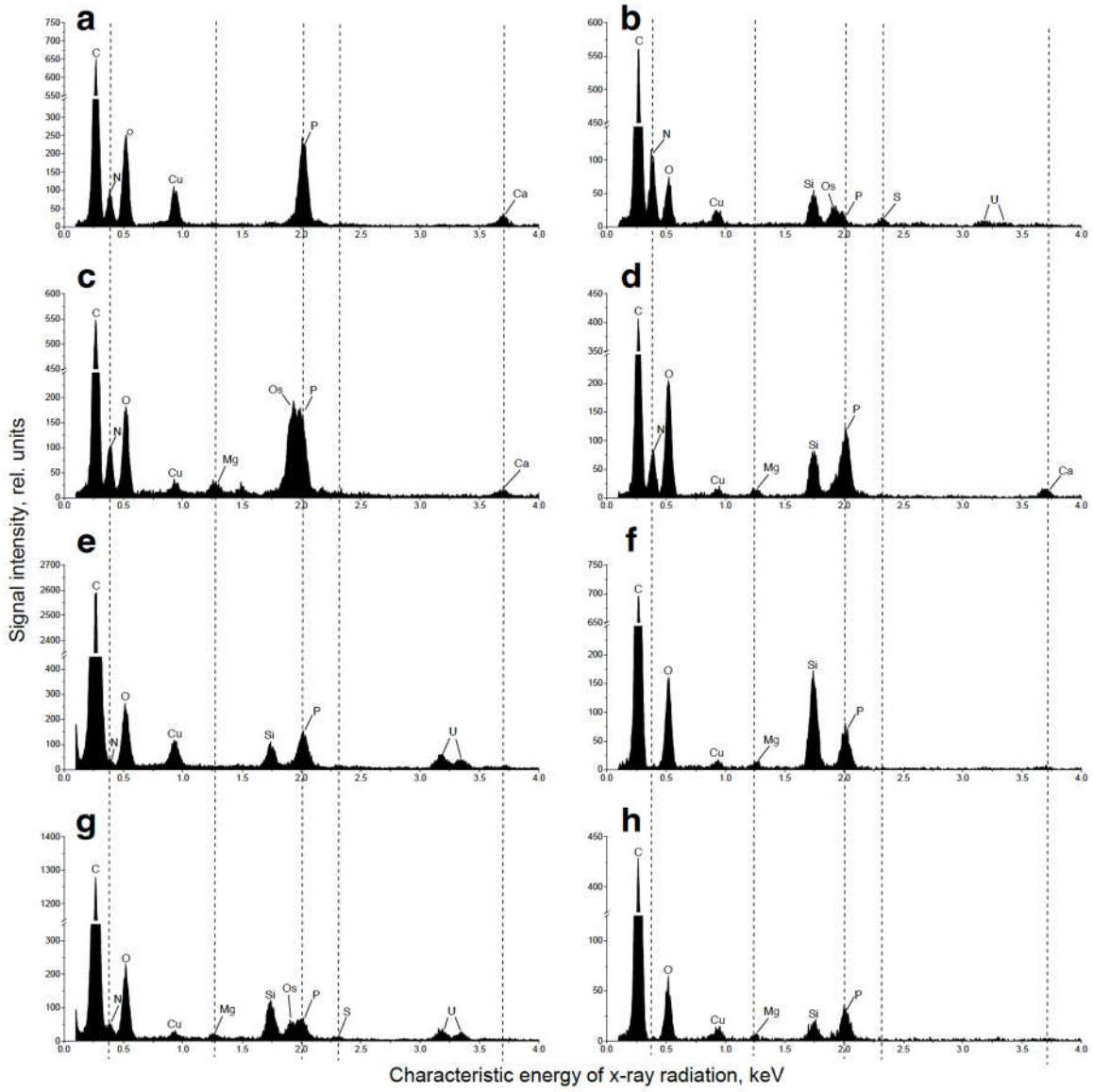

Figure 7. Representative EDX spectra of *Micractinium simplicissimum* IPPAS C-2056 cell structures potentially related with metabolism and storage of phosphorus at different phases of the experiment (see Figure 1). Vacuolar large globules in cell of the culture in the BG-11$_K$ medium (**a**), in P-starved culture (**b**), and in the cells sampled 4 h after re-feeding of the P-starved cultures with P_i (**c**); all so inclusions in cytosol (**d**), in the chloroplast stroma (**e**), the vacuolar small spherules (**f**), inclusions in the nucleus (**g**), and cell wall (**h**) after re-feeding of the P-starved cultures with P_i. All the EDX spectra possessed characteristic peaks attributable to carbon (K_α = 0.28 keV) and oxygen (K_α = 0.53 keV), the major organic constituents of biological samples and the epoxy resin they were embedded in. The spectra also contained peaks of copper (L_α = 0.93 keV) from the copper grids used for the sample mounting, as well the peaks of osmium (M_β = 1.91 keV) and uranium (M_α = 3.16 keV, M_β = 3.34 keV), used for cell fixation. The peaks of silicon (K_α = 1.74 keV) and aluminum (K_α = 1.49 keV) originate from the microscope hardware background elements.

Preprints (www.preprints.org) | NOT PEER-REVIEWED | Posted: 21 April 2023 doi:10.20944/preprints202304.0688.v1

Deprivation of P changed considerably the cell morphology and the ultrastructure (Figure 5 **b**). The amount of the cells retaining their structural integrity declined by 10–15 % (76% vs. 92% in the preculture). The thylakoids remaining in the granae were moderately expanded (the lumen width was up to 20 nm vs. 5–7 nm in the pre-culture; Figure A1a, b). The total number of starch grains decreased by 27%. At the same time, the number of oleosomes increased by 35%. Moderately electron-dense oleosomes were located on the periphery of the cell and merging forming large oleosomes (ca. 3350 nm in diameter; Figure 5 **b**). These rearrangements were in accord with the observed decline in chlorophyll (Figure 2a).

The vacuolar inclusions also displayed considerable changes during P-deprivation of the culture. They were represented by large amoeboid globules with moderately increased electron density (Figures 5 **b**, A1**c**) and sickle-shaped elongated or reticular zones of high electron density or aggregations of small particles (Figure 5 **b**) as well as by fragments of structures resembling a multiwire cable (Figure A1**d**). Small electron-dense P-containing globules were occasionally found in the vacuoles of the P-deprived cells (Table A1).

Interestingly, the DAPI-stained P-deprived cells which ceased to divide, envelopes of the sporangia, and the cell debris retained the characteristic yellow-green fluorescence (Figure 6 **c**, **d**). The EDX spectra of the structures (cell wall, different types of vacuolar inclusions, small cytoplasmic electron-opaque spherules in the stroma of chloroplast) revealed the peaks of P. The latter were also accompanied by the peaks of other elements typical of PolyP (calcium, magnesium, sodium) and the peaks of uranium or sulfur stemming from binding of the uranyl acetate (see Methods) with phosphate and sulfhydryl groups of proteins and nucleic acids (Tables A1, Figure 7). The magnitude of the P peak was lower than the N peak in the EDX spectra of the vacuolar large globules.

The analysis of ultrastructural traits of the cells after replenishment of P_i to the culture revealed diverse signs of P uptake by the cells. During the first 24 h after P_i re-feeding the proportion of the cells retaining their structural integrity increased to 88–86%, the formation of autosporangia and autospore release resumed, young cells appeared (Figures 5 c–e and 6).

The cell walls of the young cells were not stained with DAPI; accordingly, the P peak in their EDX spectra was low or absent at all. The cells in the cultures re-fed with P_i we highly heterogeneous, mostly regarding the changes of their vacuolar inclusions. Most of these inclusions assumed porous, sponge-like structure (Figures 5 **c**, **d** and A1 **e**-**g**). This process was accompanied by a decline in the magnitude of N peaks and increase in the magnitude of P peaks in the EDX spectra of these structures. In addition to this, electron-opaque globules and layers appeared inside the vacuole and on the inner surface of the tonoplast. The cells possessing these features also retained structurally intact chloroplasts (Figures 5c–e and A1 **e**-**g**). A sharp increase in the number (from several dozens to several hundred instances per cell section) of small (14–36 nm in diameter) spherules was also observed in the cytoplasm, mitochondria, nucleus, and in the dictyosomes of the Golgi apparatus. The EDX spectra of the inclusions, both vacuolar and extra-vacuolar, featured spectral details typical for PolyP including the peaks of P, magnesium, and calcium (Table A1, Figure 7). The presence of abundant PolyP was also confirmed with DAPI staining (Figure 6).

The rest of the cell population, including autospores, displayed a gross accumulation of small granules in their cytoplasm; this phenomenon was accompanied by the degradation of all organelles (mitochondria, nucleus, vacuoles with their content, chloroplasts etc.) (Figures 5 **c**–**e**, A1 **e**-**g** and A2). The amount of the destructed cells and cell debris increased with time after the P_i re-feeding from 53% at the 3rd day to 77% at the 7th day and to 92% by the 10th day. The small electron-dense spherules remained at the location of the degraded organelles and cell walls; later their number decreased from several hundreds to a several dozens of instances. Surprisingly, the degraded cells retained abundant starch grains and oleosomes.

2.4. Responses of the photosynthetic apparatus of the cells to P-starvation and re-feeding

To assess the physiological condition of the microalgal cells as manifested by the functioning of their photosynthetic apparatus (PSA) during the different phases of the experiment we recorded the

Preprints (www.preprints.org) | NOT PEER-REVIEWED | Posted: 21 April 2023 doi:10.20944/preprints202304.0688.v1

induction curves of chlorophyll *a* fluorescence and derived from the relevant JIP-test parameters (Table S1; Figure 8).

Acclimation of the culture to P deprivation was accompanied by a small decline in the potential maximal photochemical quantum yield of photosystem II, Fv/Fm. The photosynthetic performance index, PI_{ABS} was more responsive and indicator of the P deprivation stress in *M. simplicissimum* declining from ca. 0.4 to nearly zero. The flux of energy thermally dissipated by the PSA of the microalgal cells, DI_0/RC, increased very slightly, probably due to concomitant decline in the number of reaction centers manifested by the decline in chlorophyll content (not shown; see also Figure 2) whereas the parameter reflecting Stern-Volmer quenching of chlorophyll fluorescence, NPQ increased dramatically from zero (typical of unstressed cells of P-sufficient pre-culture) to 1.5. Collectively, the data on the condition of PSA (Figure 8, negative time values) suggested that the *M. simplicissimum* culture was apparently unaffected by the lack of available P in the medium for ca. 10 d (likely, due to large intracellular P reserves). Later, the cells had rapidly (over three days) acclimated to the stress, mostly by adjusting their chlorophyll content and thermal dissipation of the absorbed light energy.

Replenishment of P_i to the P-depleted *M. simplicissimum* culture triggered rapid, dramatical changes in the condition of the PSA of its cells (Figure 8, positive time values). Thus, Fv/Fm declined to the level of 0.1–0.2, and near-zero PI_{ABS} evidenced a nearly complete lack of photosynthetic activity. The NPQ parameter declined rapidly and did not increase significantly thereafter. By contrast, a tremendous increase in DI_0/RC and its variation was detected (again, likely to a gross decline in the number of reaction centers manifested by the decline of photosynthetic pigment content).

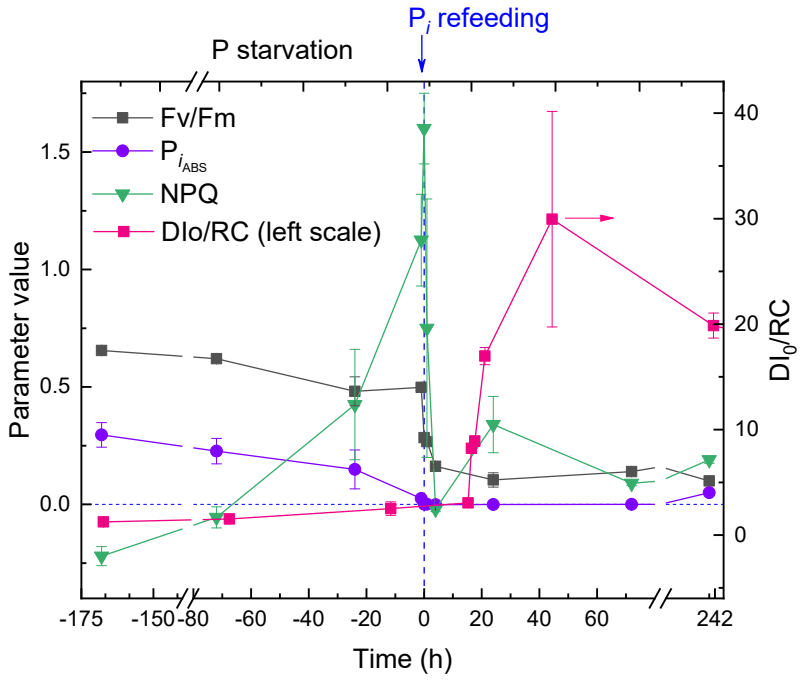

Figure 8. The kinetics of changes in JIP-test parameters (potential maximal photochemical quantum yield of photosystem II, Fv/Fm; performance index, PI_{ABS}; the flux of thermally dissipated energy flux per reaction center, DI_0/RC, left scale) and Stern-Volmer non-photochemical quenching (NPQ) in the cultures of *Micractinium simplcissimum* IPPAS C-2056 during its phosphorus starvation (negative time values) and after re-feeding of the P-starved cultures with P_i (positive time values). The moment of P_i re-feeding (t = 0 h) is specified on the graph

3. Discussion

To the best of our knowledge, this is the first report on a failure of tolerance to a high external concentration of P_i in a microalga *Micractinium simplicissimum* IPPAS C-2056 which was previously shown to be highly tolerant to this stressor [10]. We attempted to link the actual level of tolerance to

 doi:10.20944/preprints202304.0688.v1

the state of acclimation of the microalga to different P availability in the medium. We also tried to infer a plausible hypothesis explaining these apparently controversial phenomena from the physiological and ultrastructural evidence collected during this study and backed up by the current knowledge of luxury P uptake and physiological role of PolyP in microalgal cells.

Importantly, the phenomenon of failed P_i tolerance was observed only in the situation when P-starved *M. simplicissimum* culture was re-fed with P_i despite the fact that the concentration of the P_i added was far below the level potentially toxic to P-sufficient cultures of this microalga [10]. The dramatic response of *M. simplicissimum* to abrupt re-feeding with P_i was accompanied by a peculiar pattern of changes in distribution of P in the cells. There were other physiological manifestations (e.g., the variation in the photosynthetic apparatus condition) indicative of the acclimation state of the microalga. Overall, the acclimation of *M. simplicissimum* to P shortage at the first phase of the experiment manifested the onset of mild stress similarly to that during diverse stresses documented in other microalgae such as *Chlorella vulgaris* [26] or *Lobosphaera incisa* [27, 28].

Specifically, a moderate reduction of the photosynthetic apparatus has been observed as reflected by a decline in chlorophyll (Figure 2) and accumulation of carbon-rich reserve compounds (Figure 5, A1, A2) along with a depletion of P reserves in the cell. These rearrangements were accompanied with up-regulation of photoprotective mechanisms based on thermal dissipation of the observed light energy which is also typical of acclimation of microalgae to nutrient shortage [26,28,29]. Nevertheless, the cells retained their structural integrity, and their photosynthetic apparatus remained functional despite clearly observed expansion of the thylakoid lumens. Interestingly, the cells of the P-starved culture which already ceased to divide possessed a sizeable amount of PolyP granules and a N-containing matter accumulated it their vacuoles similarly to that documented in other microalgae [27,30,31]. These P reserves are obviously represented by a slowly mobilizable fraction of PolyP which frequently remains even in the P-starved cells [7,32].

After re-feeding of the P-starved culture of *M. simplicissimum* with 800 mg L^{-1} P_i, up to 20% of the added P_i was gradually removed from the medium by the cells by the 3rd day of incubation (Figure 3). Approximately 5% of the added P_i was reversibly adsorbed on the surface of the cells. DAPI staining revealed characteristic yellow fluorescence localized in the cell wall (Figure 6). This observation is in line with the previously documented ability of this strain to adsorb P_i and form P-containing nanoparticles on its surface structures [10]. This fining also corroborates previous reports on dynamic phosphorus depots in cell wall of diverse organisms including fungi, bacteria [21, 33] and microalgae [34]. As revealed by EDX spectroscopy, PolyP are characterized by co-localization with calcium, magnesium or (less frequently) potassium and sodium [35-37]. In certain cases, we also observed the P peak in combination with that of uranium. Since the uranyl cation used for the sample preparation binds to phosphate, carboxyl, and sulfhydryl groups [38], this can be a manifestation of phosphorylated proteins and nucleic acids in these cell compartments.

The amount of P internalized by the cells as well as the amount of intracellular PolyP also increased during the first four hours after re-feeding. Later, the amount of total intracellular P remained at the level of 4% of cell dry weight but the PolyP content started to decline. (Notably, the method of PolyP assay used here is optimized for long-chain PolyP, the internal PolyP content can be slightly underestimated since a part of short-chain PolyP can escape detection.) At the same time, the EDX spectral signature of PolyP was still detected in different part of the cells (Figure 7 and table A1). Starting from 1 d of incubation, the progressive signs of cell rupture were recorded. Thus, a recovery of photosynthetic apparatus would be expected normally after P_i replenishment. Instead of this we observed a complete failure of photoprotective mechanisms indicative of acute damage to the cell similar to the effect of severe stress or a toxicant in a sublethal concentration [39]. Confronting the observed effects with the reports on P_i toxicity found in the literature [23,40], we hypothesized that short-chain PolyP might be involved in the massive cell death observed in *M. simplicissimum* after its re-feeding with P_i following P-starvation.

A possible scenario of the short-chain PolyP-mediated P_i toxicity might involve the following steps. First, the P-deprived microalgal cells deploy, as a common pattern of the nutrient shortage acclimation, the mechanisms making them capable of fast P_i uptake [1,6,7,26]. At the same time, their

 doi:10.20944/preprints202304.0688.v1

capability of photosynthesis becomes impaired because of the reduction of photosynthetic apparatus (see also Figure 8). Upon re-feeding of the culture acclimated to P shortage, a large amount of P_i rapidly enters the cell. As a result, the biosynthesis of PolyP is triggered since PolyP serve as buffer for storage of P_i when it becomes available [41,42]. However, the cell acclimated to a nutrient shortage is, to a considerable extent, metabolically quiescent (in particular, its photosynthetic apparatus is down, and a large part of light energy it captures is dissipated into heat). At the same time, the biosynthesis of PolyP is very energy intensive, and this energy comes mostly from photosynthesis [43]. As the net result, these processes trigger the mass accumulation of short-chain PolyP, but the newly formed PolyP cannot be further elongated due to metabolic restrictions mentioned above. Overall, the toxic effect of the short-chain PolyP rapidly accumulated in all compartments of the cell leads to its damage and, eventually, death which was the case under our experimental conditions.

It should be noted in addition that the barrier function of the cell wall regarding P_i uptake is an important determinant of the P_i resilience in *M. simplicissimum* [10]. P_i refeeding of the culture pre-starved of P triggers cell division and hence the increase in the proportion of young cells in the cell population whose cell wall can be less efficient a barrier to P_i uptake then cell wall of mature cells. This can render the young cells more vulnerable to the surge of P_i into the cell.

The hypothesis outlined above can explain the observed phenomenon of the failed P_i tolerance since the toxic effect of short-chain PolyP initially described in yeast cells [40] was also implied in *Chlorella regularis* [23]. In these works, disorganization of cell structure has been proposed a major hallmark of elevated P_i toxicity mediated by PolyP. This hypothesis is also supported by the presence of genes encoding the PolyP polymerases from VTC family [1–3] potentially involved in the synthesis of the short-chain PolyP [39], in the genome of a closely related representative of the genus *Micractinium*, *M. conductrix* [44]. A homologue of one of these genes was putatively discovered in our pilot studies of the species used in this work, *M. simplicissimum* (in preparation).

It was also demonstrated recently that it is the PolyP that accumulates outside the cell vacuole is the main factor of PolyP-mediated toxicity of elevated external P_i [25]. One can speculate that, mechanistically, the toxicity of extra-vacuolar short-chain PolyP can interfere with protein folding and/or matrix synthesis of biomolecules. This capability of interacting with important polymeric biomolecules is attributed to PolyP as a trait of this "molecular fossil" retained from ancient times when they were potentially involved in the genesis of life [45].

Finally, we would like to underline the importance of understanding the limits of high tolerance of microalgae to elevated levels of external P_i not only for basic science, but from the practical standpoint as well. One should consider that abrupt changes of P availability can cause the normally high P_i tolerance of microalgae to fail and lead to a sudden culture crash. This is possible, particularly in the wastewater treatment facility during injection of a new portion of P-rich wastewater to P-depleted culture. Nevertheless, the toxic effects of P_i in microalgae remain quite underexplored, therefore further studies are in asset.

4. Materials and Methods

4.1. Strain and cultivation conditions

Unialgal culture of an original chlorophyte *M. simplicissimum* strain IPPAS C-2056 served as the object for this study. The pre-culture was grown in 750-mL Erlenmeyer flasks with 300 mL of modified BG-11 [10,46] medium designated below as BG-11$_K$ medium. The microalgae were cultured at 25 °C and continuous illumination of 40 μmol m^{-2} s^{-1} PAR quanta provided by daylight fluorescent tubes (Philips TL-D 36W/54-765). The cultures were mixed manually once a day.

To obtain P-depleted cultures of *M. simplicissimum*, the pre-culture cells were harvested by centrifugation (1000 × *g*, 5 min), twice washed by the BG-11$_K$ medium lacking P and resuspended in the same medium to the chlorophyll concentration and biomass content of 25 mg · L^{-1} and 0.4 g · L^{-1}, respectively in 0.6 L glass columns (4 cm internal diameter) containing 400 mL of the cell suspension. The columns were incubated in a temperature-controlled water bath at 27 °C and constant bubbling with 5% CO_2 : 95% air mixture prepared and delivered at a rate of 300 mL · min^{-1} (STP). Air passed

Preprints (www.preprints.org) | NOT PEER-REVIEWED | Posted: 21 April 2023 doi:10.20944/preprints202304.0688.v1

through 0.22 μm bacterial filter (Merck-Millipore, Billerica, MA, USA) and pure (99.999%) CO_2 from cylinders were used. A continuous illumination of 240 μmol PAR photons · m^{-2} · s^{-1} by a white light-emitting diode source as measured with a LiCor 850 quantum sensor (LiCor, Lincoln NE, United States) in the center of an empty column was used. Culture pH was measured with a bench-top pH meter pH410 with a combined electrode ESK-10601/7 (Aquilon, St.-Petersburg, Russia).

The cultures were considered to be P-depleted (having the minimum cell P quota) when the culture biomass did not increase for a consecutive three days and showed a decline in chlorophyll content (for details on monitoring of the corresponding parameters, see below). To ensure that the lack of P was the only limiting factor, the P-deprived culture was diluted with BG-11_K. medium to keep their OD_{678} below 1.5 units and the residual nitrate content was checked periodically (see below). P_i was replenished to the stationary P-depleted cultures in form of KH_2PO_4 to the final P_i concentration of 0.8 g L^{-1} and the cultures were monitored (see below) for another 10 d.

4.2. Suspension absorption spectra and pigment assay

Absorbance spectra of the microalgal cell suspension samples were recorded using Agilent Cary 300 UV-Vis spectrophotometer (Agilent, USA) equipped with a 100-mm DR30A integrating sphere of the same manufacturer and corrected for the contribution of light scattering [47]. Pigments from the cells were extracted by dimethyl sulfoxide (DMSO) and quantified spectrophotometrically using the same spectrophotometer. The content of chlorophyll *a* and *b* and total carotenoids was calculated using the equations from [48].

4.3. Biomass content determination

Dry cell weight (DCW) was determined gravimetrically. Routinely, the cells deposited on nitrocellulose filters (24 mm in diameter, 0.22 μm pore size) Millipore (Merck-Millipore, Billerica, MA, USA) were oven-dried at 105 °C to a constant weight and weighed on a 1801MP8 balance (Sartorius GmbH, Gottingen, West Germany). In certain experiments the 1.5-mL aliquots of the culture were gently centrifuged (1000 × *g*, 5 min) in pre-weighed microtubes, the supernatant was discarded, and the pellet was dried under the same conditions. The tubes with the dried cell pellet were closed and weighed on the same balance.

4.4. Assay of external and intracellular content of different P species

Concentration of P_i, along with that of nitrate, was determined in cultivation broth and cell wash liquid was assayed essentially as described in our previous work [10] using a Dionex ICS1600 (Thermo-Fisher, Sunnyvale, CA, USA) chromatograph with a conductivity detector, an IonPac AS12A (5 μm; 2 × 250 mm) anionic analytical column and an AG12A (5 μm; 2 × 50 mm) guard column according to the previously published protocol [49].

To determine the P_i adsorption of the cultures, the cells were twice washed with 15 mL BG-11_K medium lacking phosphorus. According to our previous data on independent ^{32}P-NMR control on the completeness of the P_i wash off [26], it was sufficient to remove > 99% of the adsorbed P_i. The wash liquid batches obtained from washing the same sample were pooled. The P_i content of the pooled wash liquid was assayed with HPLC as described above and confirmed independently with molybdenum blue method [50].

A modified method by Ota and Kawano [49] was used for the total intracellular P and PolyP determination. Briefly, the cell pellets from 15-mL aliquots of MA suspension after washing and removing of absorbed P were resuspended in 3-ml of distilled water. The suspended samples were divided and transferred to 2-ml microtubes: 2 ml for PolyP assay and 1 ml for total-P assay. The PolyP were extracted from cells with 5% sodium hypochlorite and precipitated with ethanol [51]. 500 μl of distilled water and 100 μl of 4% (w/v) potassium persulfate were added to the precipitated PolyP. For hydrolysis to orthophosphate, the PolyP solution was autoclaved at 121 °C for 20 min.11M For total P assay, the cell pellets were disrupted in 1 mL of distilled water with G8772 glass beads (Sigma-Aldrich, USA) and 200 μl of 4% (w/v) potassium persulfate added by vigorous mixing on a V1 vortex

 doi:10.20944/preprints202304.0688.v1

(Biosan, Latvia) for 15 min at 4 °C and subsequent autoclaving at 121 °C for 20 min. After centrifugation of the autoclaved samples (3000 × *g*, 5 min), P_i concentration was assayed in the supernatants using the molybdenum blue method [50].

4.5. Light microscopy

Light microscopy has been carried out using a Leica DM2500 microscope equipped with a digital camera Leica DFC 7000T and the light filter set AT350/50xT400lp ET500/100m (Leica, Wetzlar, Germany). PolyP inclusions were visualized using vital staining with a fluorescent dye 4′,6-diamidino-2-phenylindole (DAPI) dissolved in dimethyl sulfoxide [28]. The cells were incubated in 0.05% water solution (wt./vol.) of the dye for 5–10 min at room temperature, washed with water and studied with the microscope in brightfield mode.

4.6. Transmission electron microscopy

The microalgal samples for transmission electron microscopy (TEM) were prepared according to the standard protocol as described previously [52]. The cells were fixed in 2% v/v glutaraldehyde solution in 0.1 M sodium cacodylate buffer (pH 7.2–7.4, depending on the culture pH) and then post-fixed for 4 h in 1% (w/v) OsO_4 in the same buffer. The samples, after dehydration through graded ethanol series including anhydrous ethanol saturated with uranyl acetate, were embedded in araldite. Ultrathin sections were made with Leica EM UC7 ultratome (Leica Microsystems, Germany), mounted to the formvar-coated TEM grids, stained with lead citrate according to Reynolds [53] and examined under a JEM-1011 and JEM-1400 (JEOL, Tokyo, Japan) microscopes. All quantitative morphometric analyses were done as described previously [52]. Briefly, at least two samples from each treatment were examined on cell sections made through the cell equator or sub-equator. The subcellular structures and inclusions were counted on the sections. Linear sizes of the subcellular structure were measured on the TEM micrographs of the cell ultrathin sections ($n \geq 20$) using Fiji (ImageJ) v. 20200708-1553 software (NIH, Bethesda, MA, USA).

4.7. Analytical electron microscopy

The samples for nanoscale elemental analysis in analytical TEM using energy-dispersive X-ray spectroscopy (EDX) were prepared as described previously [29]: fixed, dehydrated, and embedded in araldite as described above excepting the staining with lead citrate. Semi-thin sections were made with Leica EM UC7 ultratome (Leica Microsystems, Germany) and examined under a JEM-2100 (JEOL, Japan) microscope equipped with a LaB_6 gun at the accelerating voltage 200 kV. Point EDX spectra were recorded using JEOL bright-field scanning TEM (STEM) module and X-Max X-ray detector system with ultrathin window capable of analysis of light elements starting from boron (Oxford Instruments, UK). The energy range of recorded spectra was 0–10 keV with a resolution of 10 eV per channel. At least 10 cells per specimen were analyzed. Spectra were recorded from different parts of electron-dense inclusions and from other (sub)compartments of microalgae cell. Spectra were processed with INKA software (Oxford instruments, UK) and presented in the range of 0.1–4 keV.

4.8 Photosynthetic activity and photoprotective mechanism assessment

Estimations of the photosynthetic activity of the microalgal cells dark-adapted for 15 min were obtained via recording Chl *a* fluorescence induction curves using FP100s portable PAM fluorometer (PSI, Czech Republic) using the built-in protocol supplied by the manufacturer. The recorded curves were processed by the built-in software of the fluorometer and the JIP-test parameters indicative of the functional condition of the photosynthetic apparatus of the microalgal cells were calculated (Table S1, see also [54,55]).

 doi:10.20944/preprints202304.0688.v1

4.9. Statistical treatment

Under the specified conditions, three independent experiments were carried out for each treatment repeated in duplicate columns. The average values (n = 6) and corresponding standard deviation are shown unless stated otherwise.

5. Conclusions

Microalgae including the *M. simplicicssimum* strain studied here are resilient to very high concentration of exogenic P_i. As it turned out in this work, this resilience fails after abrupt re-supplementation of P_i to the culture pre-starved of P. This was the case even if P_i was re-supplemented at the concentration far below the level which can be toxic to the P-sufficient culture. The obtained evidence suggests that this effect can be mediated by the rapid formation of the potentially toxic short-chain PolyP following the mass influx of P_i into the P-starved cell. A possible reason for this is that the preceding P starvation impairs the capacity of the cell of converting the newly absorbed P_i into a "safe" storage form of long-chain PolyP. We believe that findings of this study can help to avoid sudden culture crashes are of potential significance for development of algae-based technologies for efficient bioremoval of P from P-rich waste streams.

Supplementary Materials: Table S1: The JIP-test parameters used for monitoring of the microalgal cultures in the present work; Table S2: Elemental composition and localization the inclusions in the degraded cells *Micractinium simplicissimum* IPPAS C-2056.

Author Contributions: Conceptualization, A.S. and O.G.; methodology, I.S., S.V. and L.S.; validation, O.G., and E.L.; formal analysis, P.S. and S.V.; investigation, I.S., L.S., O.C., K.S., O.B., O.G., P.S. and P.Z; writing—original draft preparation, A.S. and O.G.; writing—review and editing, A.S., E.L. and O.G.; visualization, O.G. and P.Z.; supervision, E.L.; project administration, A.S. and E.L.; funding acquisition, A.S, S.V. All authors have read and agreed to the published version of the manuscript.

Funding: This research was funded in part by the Russian Science Foundation (grant 23-74-00037, the spectral and PAM measurements; grant 23-24-00122, electron microscopy studies). The rest investigations were supported by Ministry of Science and Higher Education of Russian Federation (grant 075-15-2021-1396).

Data Availability Statement: The data are available from the corresponding author on a reasonable request.

Acknowledgments: The EM studies were carried out at the Shared Research Facility "Electron microscopy in life sciences" at Moscow State University (Unique Equipment "Three-dimensional electron microscopy and spectroscopy"). Photosynthetic activity of microalgae was estimated using the Shared Research Facility "Phototrophic Organism Phenotyping." The support of the scientific and educational school of LMSU "Molecular technologies of living systems and synthetic biology" is appreciated.

Conflicts of Interest: The authors declare no conflict of interest. The funders had no role in the design of the study; in the collection, analyses, or interpretation of data; in the writing of the manuscript; or in the decision to publish the results.

Preprints (www.preprints.org) | NOT PEER-REVIEWED | Posted: 21 April 2023 doi:10.20944/preprints202304.0688.v1

Appendix A

Table A1. Elemental composition and localization the inclusions in cells *Micractinium simplicissimum* IPPAS C-2056 which had retained their integrity (for explanation, see text)

Medium type or time after P_i re-feeding	**Cell wall**	**Cytosol**	**Vacuole**		**Chloroplast stroma**	**Nucleus**
			Small spherules	Large globules		
BG-11K	**P†, Fe	P-N, P† P-Ca†	P / P†	P-N-Ca†, P-N-Mg-Ca	P-N†, P-Mg†	P-N*
P-free medium	P / P†, Fe, P-S, P-Mg-Ca†, N-S†	P-N-Mg-Ca-Na†	P-N†, P-Mg-Ca†, P-N-Mg-Ca†, P	N-P-S, N-P†, P-N-Mg-Ca†	P / P†	P-N*, P-N-Mg*
4 h*	Fe-S, P-N-S, S-N, N-P-S-Mg P-S-Mg-Ca-U	P-N-Ca-Mg† P-Mg† P-N	P-Mg-Ca, P-N-Mg-Ca†, P-N-Ca, P-Mg†, P-N-Mg† P / P†	P-N-Na-Ca, P-N-Mg-Ca, P-N / P-N †, P-N-Ca P-Mg-Ca†	P-N†, P	P-N*, P-S*, P-N-S-Mg*
24 h	Fe, P-Fe, P-N-S-Fe, P-Ca / P-Ca †, P-N† P-Mg-Ca†, P-Mg-K-Ca P-S-Ca† P-Mg	P-Mg, P-Ca P-Mg-Ca, P-N-S-Mg-Ca	P-Mg P-Mg-Ca† P-N-Ca-Mg† P-N-Ca P-N-Mg	P-N-Mg	P-N-S†, P† Fe	P-N* P-Mg-Ca P-K-Mg-Ca
72 h	P-Ca-Fe-Mg Fe	P	P-N-Mg-Na-Ca† P-N-Mg-Ca† P-N-Mg† P-Mg-Ca†	P-N-Mg-Ca	P-Mg-K†, P-Ca† P-Na	P
168 – 240 h	P-Ca	P-N-Mg, P-N, P	P-N-Mg-Ca, P-N-Mg	ND	P†, P-S†, P-S-Ca† P-N-Mg P-Ca†	ND

*Time after re-feeding of the P-starved cultures with P_i.

**Elements are ordered according to a decrease in the magnitude of the corresponding element peak in the EDX spectrum.

†The EDX spectrum possessed the peak of uranium (U).

Preprints (www.preprints.org) | NOT PEER-REVIEWED | Posted: 21 April 2023 doi:10.20944/preprints202304.0688.v1

ND—no data.

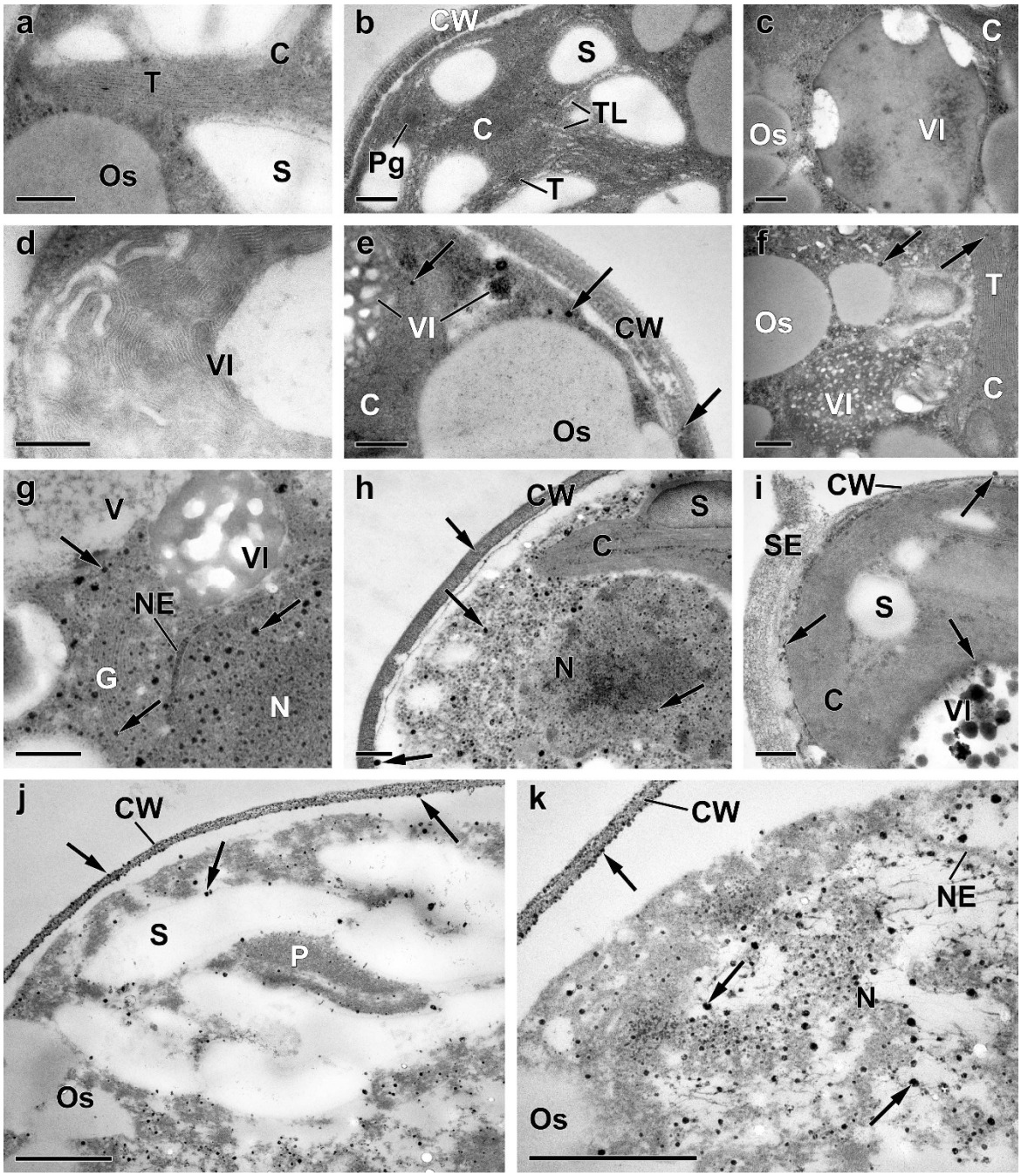

Figure A1. Representative transmission electron micrographs of *Micractinium simplcissimum* IPPAS C-2056 cells reflecting their condition at different phases of the experiment (for more details, see Figure 1 and Methods). The micrographs of P-sufficient pre-culture cells (**a**), P-starved cells (**b-d**), as well as of cells sampled 4 h (**e-g**), 24 h (h), and 72 h (**i-k**) after re-feeding of the P-starved cultures with Pi are shown. C, chloroplast; CW, cell wall; G, dictyosomes of Golgi apparatus; N, nucleus; NE, nuclear envelope; Os, oleosome; P, pyrenoid, Pg, plastoglobuli; S, Starch granule; SE, sporangium envelope; T, thylakoids; TL, thylakoid lumen; V, vacuole; VI, vacuolar inclusion. The arrows point to (i) the electron-opaque particles located on the surface of or within the cell, (ii) to their clusters adsorbed on the cell surface, and (iii) to the spherules in the cytoplasm, the nucleus, and the destructed chloroplast. Scale bars: 0.2 μm (**a-i**), 0.5 μm (**j-k**).

Preprints (www.preprints.org) | NOT PEER-REVIEWED | Posted: 21 April 2023 doi:10.20944/preprints202304.0688.v1

Appendix B

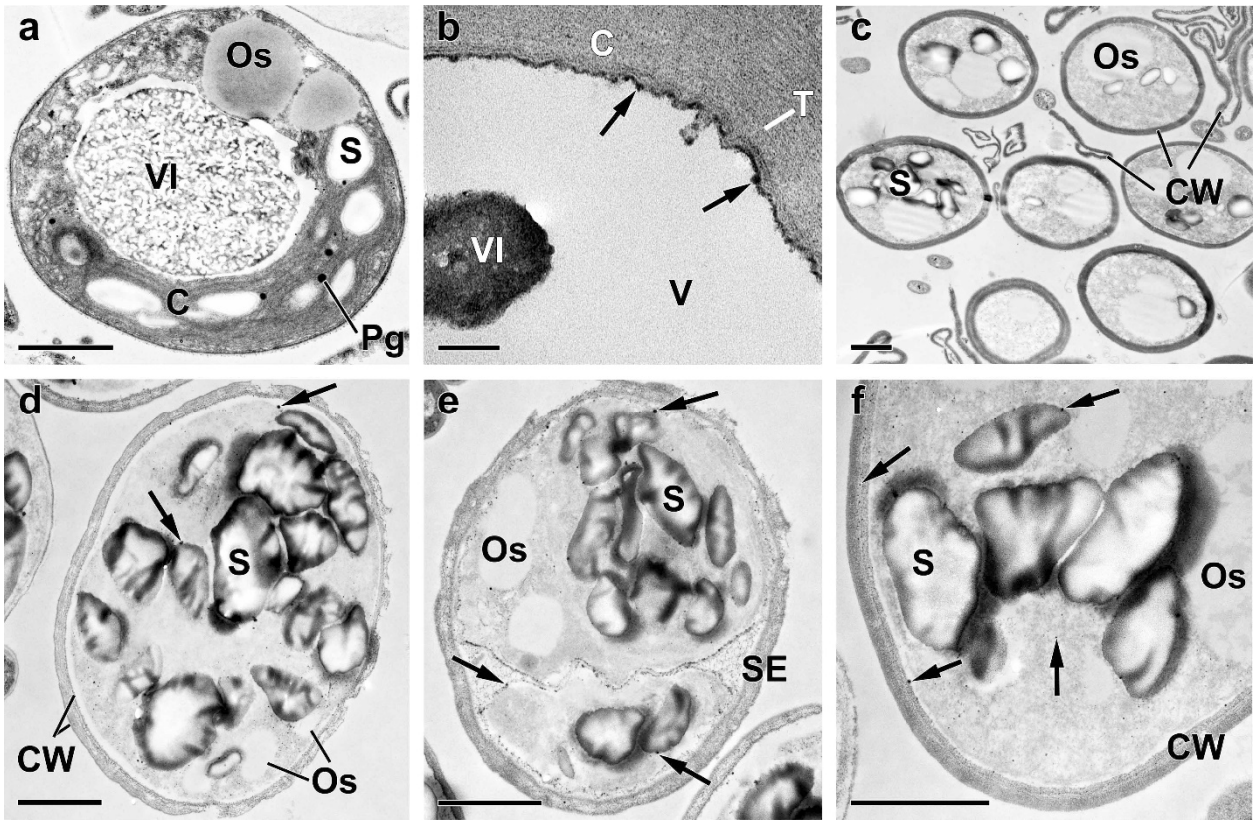

Figure A2. Representative transmission electron micrographs of *Micractinium simplcissimum* IPPAS C-2056 cells reflecting their condition at different phases of the experiment (for more details, see Figure 1 and Methods). The micrographs of cells (**a**-**d**, **f**) and sporangium (**e**) sampled 168 h (**a**-**c**) and 240 h (**d**-**f**) after re-feeding of the P-starved cultures with P_i are shown. C, chloroplast; CW, cell wall; Os, oleosome; Pg, plastoglobuli; S, starch granule; SE, sporangium envelope; T, thylakoids; V, vacuole; VI, vacuolar inclusion. The arrows point to (i) the electron-opaque particles located on the surface of or within the cell wall, (ii) to the inner surface of the tonoplast and (iii) to the spherules in the cytoplasm, and the destructed chloroplast. Scale bars: 1 μm (**a**, **c**-**f**), 0.1 μm (**b**).

References

1. Solovchenko, A.E.; Ismagulova, T.T.; Lukyanov, A.A.; Vasilieva, S.G.; Konyukhov, I.V.; Pogosyan, S.I.; Lobakova, E.S.; Gorelova, O.A. Luxury phosphorus uptake in microalgae. *Journal of Applied Phycology* **2019**, *31*, 2755-2770.
2. Solovchenko, A.; Verschoor, A.M.; Jablonowski, N.D.; Nedbal, L. Phosphorus from wastewater to crops: An alternative path involving microalgae. *Biotechnology advances* **2016**, *34*, 550–564.
3. Dyhrman, S.T. Nutrients and their acquisition: phosphorus physiology in microalgae. In *The physiology of microalgae*, Springer: 2016; pp. 155-183.
4. de Mazancourt, C.; Schwartz, M.W. Starve a competitor: evolution of luxury consumption as a competitive strategy. *Theoretical Ecology* **2012**, *5*, 37-49.
5. Watanabe, M.; Kohata, K.; Kunugi, M. Phosphate accumulation and metabolism by *Heterosigma akashiwo* (Raphidophyceae) during diel vertical migration in a stratified microcosm. *Journal of phycology* **1988**, *24*, 22-28.
6. Cembella, A.; Antia, N.; Harrison, P.; Rhee, G.-Y. The Utilization of Inorganic and Organic Phosphorous Compounds as Nutrients by Eukaryotic Microalgae: A Multidisciplinary Perspective: Part 2. *Critical Reviews in Microbiology* **1984**, *11*, 13-81.
7. Cembella, A.D.; Antia, N.J.; Harrison, P.J. The utilization of inorganic and organic phosphorous compounds as nutrients by eukaryotic microalgae: A multidisciplinary perspective: Part I. *Critical reviews in microbiology* **1982**, *10*, 317-391.
8. Haneklaus, S.; Bloem, H.; Schnug, E. Hungry Plants—A Short Treatise on How to Feed Crops under Stress. *Agriculture* **2018**, *8*, doi:10.3390/agriculture8030043.
9. Rhee, G.-Y. A continuous culture study of phosphate uptake, growth rate and polyphosphate in *Scenedesmus* sp. *Journal of Phycology* **1973**, *9*, 495-506.
10. Lobakova, E.S.; Selyakh, I.O.; Semenova, L.R.; Scherbakov, P.N.; Fedorenko, T.A.; Chekanov, et al. Hints for understanding microalgal phosphate-resilience from *Micractinium simplicissimum* IPPAS C-2056 (Trebouxiophyceae) isolated from a phosphorus-polluted site. *Journal of Applied Phycology* **2022**, *34*, 2409-2422.
11. Brown, N.; Shilton, A. Luxury uptake of phosphorus by microalgae in waste stabilisation ponds: current understanding and future direction. *Reviews in Environmental Science and Bio/Technology* **2014**, *13*, 321-328, doi:10.1007/s11157-014-9337-3.
12. Smil, V. Phosphorus in the environment: natural flows and human interferences. *Annual review of energy and the environment* **2000**, *25*, 53-88.
13. Ketchum, B.H. The absorption of phosphate and nitrate by illuminated cultures of *Nitzschia closterium*. *American Journal of Botany* **1939**, 399-407.
14. Eixler, S.; Karsten, U.; Selig, U. Phosphorus storage in *Chlorella vulgaris* (Trebouxiophyceae, Chlorophyta) cells and its dependence on phosphate supply. *Phycologia* **2006**, *45*, 53-60.
15. Cordell, D.; White, S. Life's Bottleneck: Implications of Global Phosphorus Scarcity and Pathways for a Sustainable Food System. *Annual Review of Environment and Resources* **2014**, *39*.
16. Ronga, D.; Biazzi, E.; Parati, K.; Carminati, D.; Carminati, E.; Tava, A. Microalgal Biostimulants and Biofertilisers in Crop Productions. *Agronomy* **2019**, *9*, doi:10.3390/agronomy9040192.
17. de Siqueira Castro, J.; Calijuri, M.L.; Ferreira, J.; Assemany, P.P.; Ribeiro, V.J. Microalgae based biofertilizer: A life cycle approach. *Science of The Total Environment* **2020**, 10.1016/j.scitotenv.2020.138138, doi:10.1016/j.scitotenv.2020.138138.

18. Mulbry, W.; Westhead, E.K.; Pizarro, C.; Sikora, L. Recycling of manure nutrients: use of algal biomass from dairy manure treatment as a slow release fertilizer. *Bioresource Technology* **2005**, *96*, 451-458.
19. Slocombe, S.P.; Zúñiga-Burgos, T.; Chu, L.; Wood, N.J.; Camargo-Valero, M.A.; Baker, A. Fixing the Broken Phosphorus Cycle: Wastewater Remediation by Microalgal Polyphosphates. *Frontiers in Plant Science* **2020**, *11*, doi:10.3389/fpls.2020.00982.
20. Pittman, J.K.; Dean, A.P.; Osundeko, O. The potential of sustainable algal biofuel production using wastewater resources. *Bioresource Technology* **2011**, *102*, 17-25, doi:DOI: 10.1016/j.biortech.2010.06.035.
21. Kulaev, I.; Vagabov, I.; Kulakovskaya, T. *The Biochemistry of Inorganic Polyphosphates*, 2 ed.; John Wiley & Sons, Ltd: Chichester, England, 2004.
22. Xie, L.; Jakob, U. Inorganic polyphosphate, a multifunctional polyanionic protein scaffold. *Journal of Biological Chemistry* **2019**, *294*, 2180-2190.
23. Li, Q.; Fu, L.; Wang, Y.; Zhou, D.; Rittmann, B.E. Excessive phosphorus caused inhibition and cell damage during heterotrophic growth of *Chlorella regularis*. *Bioresource Technology* **2018**, *268*, 266-270, doi:10.1016/j.biortech.2018.07.148.
24. Fu, L.; Li, Q.; Yan, G.; Zhou, D.; Crittenden, J.C. Hormesis effects of phosphorus on the viability of Chlorella regularis cells under nitrogen limitation. *Biotechnol Biofuels* **2019**, *12*, 121, doi:10.1186/s13068-019-1458-z.
25. McCarthy, L.; Abramchuk, I.; Wafy, G.; Denoncourt, A.; Lavallée-Adam, M.; Downey, M. Ddp1 Cooperates with Ppx1 to Counter a Stress Response Initiated by Nonvacuolar Polyphosphate. *mBio* **2022**, 10.1128/mbio.00390-22, doi:10.1128/mbio.00390-22.
26. Solovchenko, A.; Khozin-Goldberg, I.; Selyakh, I.; Semenova, L.; Ismagulova, T.; Lukyanov, A.; Mamedov, I.; Vinogradova, E.; Karpova, O.; Konyukhov, I., et al. Phosphorus starvation and luxury uptake in green microalgae revisited. *Algal Research* **2019**, *43*, 101651.
27. Vasilieva, S.; Lobakova, E.; Gorelova, O.; Baulina, O.; Scherbakov, P.; Chivkunova, O.; Semenova, L.; Selyakh, I.; Lukyanov, A.; Solovchenko, A. Photosynthetic and ultrastructural responses of the chlorophyte Lobosphaera to the stress caused by a high exogenic phosphate concentration. *Photochemical & Photobiological Sciences* **2022**, *21*, 2035-2051.
28. Kokabi, K.; Gorelova, O.; Ismagulova, T.; Itkin, M.; Malitsky, S.; Boussiba, S.; Solovchenko, A.; Khozin-Goldberg, I. Metabolomic foundation for differential responses of lipid metabolism to nitrogen and phosphorus deprivation in an arachidonic acid-producing green microalga. *Plant Science* **2019**, *283*, 95-115.
29. Gorelova, O.; Baulina, O.; Ismagulova, T.; Kokabi, K.; Lobakova, E.; Selyakh, I.; Semenova, L.; Chivkunova, O.; Karpova, O.; Scherbakov, P.; et al. Stress-induced changes in the ultrastructure of the photosynthetic apparatus of green microalgae. *Protoplasma* **2019**, *256*, 261–277.
30. Shebanova, A.; Ismagulova, T.; Solovchenko, A.; Baulina, O.; Lobakova, E.; Ivanova, A.; Moiseenko, A.; Shaitan, K.; Polshakov, V.; Nedbal, L., et al. Versatility of the green microalga cell vacuole function as revealed by analytical transmission electron microscopy. *Protoplasma* **2017**, *254*, 1323–1340.
31. Ismagulova, T.; Shebanova, A.; Gorelova, O.; Baulina, O.; Solovchenko, A. A new simple method for quantification and locating P and N reserves in microalgal cells based on energy-filtered transmission electron microscopy (EFTEM) elemental maps. *PloS one* **2018**, *13*, e0208830.
32. Miyachi, S.; Kanai, R.; Mihara, S.; Miyachi, S.; Aoki, S. Metabolic roles of inorganic polyphosphates in *Chlorella* cells. *Biochimica et Biophysica Acta* **1964**, *93*, 625-634.

33. Werner, T.P., Amrhein, N., Freimoser, F.M. Specific localization of inorganic polyphosphate (poly P) in fungal cell walls by selective extraction and immunohistochemistry. *Fungal Genetics and Biology* **2007**, *44*, 845-852.
34. Werner, T.P., Amrhein, N., Freimoser, F.M. Inorganic polyphosphate occurs in the cell wall of *Chlamydomonas reinhardtii* and accumulates during cytokinesis. *BMC Plant Biology* **2007**, *7*, 1-11.
35. Ruiz, F.A.; Marchesini, N.; Seufferheld, M.; Govindjee; Docampo, R. The Polyphosphate bodies of *Chlamydomonas reinhardtii* possess a proton-pumping pyrophosphatase and are similar to acidocalcisomes. *Journal of Biological Chemistry* **2001**, *276*, 46196-46203.
36. Docampo, R.; de Souza, W.; Miranda, K.; Rohloff, P.; Moreno, S.N. Acidocalcisomes? Conserved from bacteria to man. *Nature Reviews Microbiology* **2005**, *3*, 251-261.
37. Docampo, R.; Huang, G. Acidocalcisomes of eukaryotes. *Current Opinion in Cell Biology* **2016**, *41*, 66-72.
38. Geyer, G. Ultrahistochemie: histochemische Arbeitsvorschriften fuïr die Elektronenmikroskopie. Jena, Stuttgart: VEB Gustav Fischer Verlag, 1973.
39. Solovchenko, A.E.; Vasilieva, S.G.; Zaitsev, P.; Lukyanov, A.A.; Skripnikova, E.V.; Antal, T.K. Approaches to rapid screening of pharmaceutical xenobiotic effects on microalgae via monitoring of photosynthetic apparatus condition. *Journal of Applied Phycology* **2022**, *34*, 353-361.
40. Gerasimaite, R.; Sharma, S.; Desfougeres, Y.; Schmidt, A.; Mayer, A. Coupled synthesis and translocation restrains polyphosphate to acidocalcisome-like vacuoles and prevents its toxicity. *J Cell Sci* **2014**, *127*, 5093-5104, doi:10.1242/jcs.159772.
41. Desfougeres, Y.; Gerasimaite, R.U.; Jessen, H.J.; Mayer, A. Vtc5, a Novel Subunit of the Vacuolar Transporter Chaperone Complex, Regulates Polyphosphate Synthesis and Phosphate Homeostasis in Yeast. *J Biol Chem* **2016**, *291*, 22262-22275, doi:10.1074/jbc.M116.746784.
42. Gerasimaitė, R.; Mayer, A. Enzymes of yeast polyphosphate metabolism: structure, enzymology and biological roles. *Biochemical Society Transactions* **2016**, *44*, 234-239.
43. Aitchison, P.; Butt, V. The relation between the synthesis of inorganic polyphosphate and phosphate uptake by *Chlorella vulgaris*. *Journal of Experimental Botany* **1973**, *24*, 497-510.
44. Arriola, M.B.; Velmurugan, N.; Zhang, Y.; Plunkett, M.H.; Hondzo, H.; Barney, B.M. Genome sequences of *Chlorella sorokiniana* UTEX 1602 and *Micractinium conductrix* SAG 241.80: implications to maltose excretion by a green alga. *The plant journal* **2018**, 93, 566-586.
45. Achbergerová, L.; Nahálka, J. Polyphosphate-an ancient energy source and active metabolic regulator. *Microb Cell Fact* **2011**, *10*, 14170-14175.
46. Stanier, R.; Kunisawa, R.; Mandel, M.; Cohen-Bazire, G. Purification and properties of unicellular blue-green algae (order Chroococcales). *Microbiology and Molecular Biology Reviews* **1971**, *35*, 171-205.
47. Merzlyak, M.N.; Naqvi, K.R. On recording the true absorption spectrum and the scattering spectrum of a turbid sample: application to cell suspensions of the cyanobacterium *Anabaena variabilis*. *J Photochem Photobiol B* **2000**, *58*, 123-129.
48. Solovchenko, A.; Merzlyak, M.; Khozin-Goldberg, I.; Cohen, Z.; Boussiba, S. Coordinated carotenoid and lipid syntheses induced in *Parietochloris incisa* (Chlorophyta, Trebouxiophyceae) mutant deficient in Δ5 desaturase by nitrogen starvation and high light. *Journal of Phycology* **2010**, *46*, 763-772, doi:10.1111/j.1529-8817.2010.00849.x.
49. Solovchenko, A.; Pogosyan, S.; Chivkunova, O.; Selyakh, I.; Semenova, L.; Voronova, E.; Scherbakov, P.; Konyukhov, I.; Chekanov, K.; Kirpichnikov, M., et al. Phycoremediation of alcohol distillery wastewater with a novel *Chlorella sorokiniana* strain cultivated in a photobioreactor monitored on-line

via chlorophyll fluorescence. *Algal Research-Biomass Biofuels and Bioproducts* **2014**, *6*, 234-241, doi:10.1016/j.algal.2014.01.002.

50. Ota, S.; Kawano, S. Extraction and Molybdenum Blue-based Quantification of Total Phosphate and Polyphosphate in *Parachlorella*. *Bio-protocol* **2017**, *7*, e2539, doi:10.21769/BioProtoc.2539.
51. Sutherland, I.; Wilkinson, J. Chapter IV Chemical Extraction Methods of Microbial Cells. In *Methods in microbiology*, Elsevier: 1971; Vol. 5, pp. 345-383.
52. Gorelova, O.; Baulina, O.; Solovchenko, A.; Selyakh, I.; Chivkunova, O.; Semenova, L.; Scherbakov, P.; Burakova, O.; Lobakova, E. Coordinated rearrangements of assimilatory and storage cell compartments in a nitrogen-starving symbiotic chlorophyte cultivated under high light. *Archives of Microbiology* **2015**, *197*, 181-195, doi:10.1007/s00203-014-1036-5.
53. Reynolds, E. The use of lead citrate at high pH as an electron-opaque stain in electron microscopy. *The Journal of Cell Biology* **1963**, *17*, 208.
54. Strasser, R.; Tsimilli-Michael, M.; Srivastava, A. Analysis of the chlorophyll *a* fluorescence transient. In *Chlorophyll a fluorescence: a signature of photosynthesis*, *Papageorgiou, G., Govindjee*, Eds. Springer: 2004; pp. 321–362.
55. Solovchenko, A.; Lukyanov, A.; Vasilieva, S.; Lobakova, E. Chlorophyll fluorescence as a valuable multitool for microalgal biotechnology. *Biophysical Reviews* **2022**, 10.1007/s12551-022-00951-9, doi:10.1007/s12551-022-00951-9.

Preprints (www.preprints.org) | NOT PEER-REVIEWED | Posted: 21 April 2023 doi:10.20944/preprints202304.0688.v1

Table S1. The JIP-test parameters used for monitoring of the microalgal cultures in the present work (according to [54,55]).

Parameter	Description
F_O, F_J, F_{300}, F_m	Fluorescence yield at the points O (minimal fluorescence, when all PS II reaction centers, RC are open), J (2 ms), at 300 μs (K-step), and at the point of the maximum of OJIP, M, when all PS II RC are closed
PS II $Q_y = \varphi_{P_0} = \frac{F_m - F_O}{F_m} = \frac{F_V}{F_m}$	Maximum potential quantum yield of primary photochemistry in photosystem II
NPQ = $\frac{F_m}{F_m'} - 1$	A non-photochemical quenching parameter according to Stern-Volmer
$\psi_0 = 1 - \frac{F_J - F_O}{F_M - F_O}$	The probability of electron transfer from PS II to PQ pool
$M_0 = 4\frac{F_{300} - F_O}{F_M - F_O}$	An approximation of the initial slope of OJIP attributed to QA reduction
$\phi_{D_0} = \frac{F_O}{F_M}$	Quantum yield of energy dissipation
$\phi_{E_0} = \psi_0\left(1 - \frac{F_O}{F_M}\right)$	Quantum yield of electron transport
ABS/RC = $M_0 \cdot \frac{1}{V_J} \cdot \frac{1}{\varphi_{P_0}}$	Absorbed energy flux per RC
TR_0/RC = $M_0 \cdot \frac{1}{V_J}$	Trapped energy flux per RC
DI_0/RC = ABS/RC - TR_0/RC	Thermally dissipated energy flux per RC
PI_{ABS} = ABS/RC $\cdot \left(\frac{\varphi_{P_0}}{1-\varphi_{P_0}}\right) \cdot \left(\frac{\psi_0}{1-\psi_0}\right)$	Performance index expressed on the light absorption basis

Preprints (www.preprints.org) | NOT PEER-REVIEWED | Posted: 21 April 2023 doi:10.20944/preprints202304.0688.v1

Table S2. Elemental composition and localization the inclusions in the ruptured cells *Micractinium simplicissimum* IPPAS C-2056 (for explanation, see text)

Medium type or time after P_i re-feeding	Cell wall	Cytosol	Vacuole		Chloroplast stroma	Nucleus
			Small spherules	Large globules		
BG-11$_K$	ND	ND	ND	ND	ND	ND
P-free medium	ND	ND	ND	ND	ND	ND
4 h*	ND	ND	ND	ND	ND	ND
24 h	**Fe, Fe-P, Fe-P-S, P-Ca-Mg, P-Ca, P-Mg, P†	P-Na-Mg-Ca, P-N-Mg	P-Mg-Ca† P-N-S-Ca-Mg P-N-Mg	P-N-Mg, P-N-Ca	P-S†, P-Mg-Ca	P†
72 h	Fe, P, S, P-Fe-Na-Ca	ND	ND	ND	ND	ND
168–240 h	P	P-N-Mg, P-N, P	P-Na-Mg, P-Na-Mg-Ca	ND	P-N	ND

*Time after re-feeding of the P-starved cultures with P_i.

**Elements are ordered according to an increase in the magnitude of the corresponding element peak in the EDX spectrum.

†The EDX spectrum possessed the peak of uranium (U).

ND—no data.